Spatial and Temporal Variation in Erosion and Accumulation of the Subaqueous Yellow River Delta (1976–2004)

Authors: Xing, Guopan, Wang, Houjie, Yang, Zuosheng, and Bi, Naishuang

Source: Journal of Coastal Research, 74(sp1) : 32-47

Published By: Coastal Education and Research Foundation

URL: https://doi.org/10.2112/SI74-004.1

Journal of Coastal Research	SI	74	32–47	Coconut Creek, Florida	2016

Spatial and Temporal Variation in Erosion and Accumulation of the Subaqueous Yellow River Delta (1976–2004)

Guopan Xing[‡], Houjie Wang[‡], Zuosheng Yang[‡], and Naishuang Bi[‡*]

[‡] College of Marine Geosciences
Ocean University of China
Qingdao, Shandong 266100, P. R. China

www. cerf-jcr. org

www. JCRonline. org

ABSTRACT

Xing, G. P.; Wang, H. J.; Yang, Z. S., and Bi, N. S., 2016. Spatial and temporal variation in erosion and accumulation of the subaqueous Yellow River Delta (1976–2004). *In*: Harff, J. and Zhang, H. (eds.), *Environmental Processes and the Natural and Anthropogenic Forcing in the Bohai Sea, Eastern Asia. Journal of Coastal Research*, Special Issue, No. 74, pp. 32–47. Coconut Creek (Florida), ISSN 0749–0208.

Yellow River Delta (YRD), one of the most heavily human-influenced delta systems, had undergone dramatic changes since 1976. To determine the erosion and accretion pattern of the subaqueous YRD, bathometry data as well as the sediment discharge from the Lijin station over the period of 1976 to 2004 were analyzed. The erosion and accretion pattern of the subaqueous YRD was delineated by 1) the northern abandoned delta lobe, consisted of the heavily eroded Diaokou (DK) and Shenxiangou (SXG) lobes; 2) the active delta lobe, comprised of Qingshuigou (QSG) and Q8 lobes and featuring fast progradation; 3) the Laizhou Bay (LZB) with slight accumulation. Three stages were summarized based on the evolution of the northern abandoned delta lobe. During 1976–1980, the northern abandoned delta was severely eroded due to the cutoff of sediment supply. As the subaqueous slope became gentler during 1980–1996, the deeper part of the subaqueous delta turned into slight accretion state while the shallow part continued to be eroded. However, the erosion rate of the northern delta slowed down to a relatively balanced state during 1996–2004. Meanwhile, the development of the active delta lobe was a product of riverine sediment supply, channel geometry and estuarine hydrodynamics. Multi-depocenter was formed along the coastal area of the active subaqueous delta during 1976–1980, when multiple channels were active for sediment transportation. As the main river channel developed, the depocenter progradated eastward with an exceptional high accumulation rate during 1980–1985. The progradation direction turned southeastward with a lower accumulation rate during 1985–1996. Then, the depocenter shifted to the newly formed Q8 river mouth after a channel diversion in 1996, leaving the QSG river mouth in severe erosion. The channel diversion also caused erosion at the offshore area in LZB, where slight accumulation dominated before 1996. The erosion and accumulation pattern of the subaqueous YRD showed significant spatial and temporal variability during 1976–2004. A comprehensive understanding of their driven mechanisms would be critical for the prediction of the evolution of the YRD in the context of global change.

ADDITIONAL INDEX WORDS: *Yellow River Delta, erosion and accumulation, spatial and temporal variation, dominant factors.*

INTRODUCTION

Deltas, home to millions of people, are continually responding to the interaction between lands and oceans (Wright, 1985). As the major form of coastal lowland, the evolution of deltas critically depend on such factors as the water and sediment discharge of river systems, sea-level variation, and physical-oceanographic regimes of the coastal seas into which the river-born sediment are debouched (Wright and Nittrouer, 1995). As a result, river deltas are sensitive to the global climate change and human activities (Bianchi and Allision, 2009). Over the last century, many deltas are subject to the risk of inundation due to the reduction of river-born sediment supply caused by climate change and human activities, especially the heavily populated megadeltas in Asia, where the emerging economies are extending their footprints on the delta systems and transforming them into increasingly fragile coastal regions (Overeem and Syvitski, 2009; Syvitski, *et al.*, 2009).

In history, the Yellow River (Huanghe) (YR) was characterized by a high concentration of sediment, tremendous sediment load, and frequent lateral delta lobe shift (Saito *et al.*, 2001). However, since 1950, the sediment load of the YR has experienced stepwise decrease from annual sediment load of 1.08 Gt/yr to 0.15 Gt/yr during 2000–2005 (Wang *et al.*, 2007). The weakening feeding river has made the YRD a vulnerable area to disastrous ocean forces. Moreover, the YRD has become an increasingly human-regulated system via reservoirs, dams, and levees.

DOI: 10.2112/SI74–004.1 received (11 February 2015); accepted in revision (31 October 2015).

*Corresponding author; binaishuang@ouc.edu.cn

Many studies have been dedicated to the YRD erosion and accretion process. The erosion problems of the abandoned YRD lobes gradually aroused people's concern after the deltaic channel shift from the Diaokou (DK) channel to Qingshuigou (QSG) channel. The evolution of the erosion process has been studied (Li *et al.*, 2000; Liu, *et al.*, 2002; Ying, *et al.*, 2007) and formulated as a process controlled by the interaction of sediment load of the YR, waves (Wang *et al.*, 2010), tidal current (Chen *et al.*, 2005), geomorphology (Chen *et al.*, 2005), and the sediment geotechnical strength (Jia *et al.*, 2011, Ying *et al.*, 2007). Meanwhile, the fast progradation of the active delta lobe has been formulated as a process characterized by hyperpycnal flow (Li *et al.*, 1998; Wang *et al.*, 2010; Wright *et al.*, 1986) and shear front (Li *et al.*, 2001; Qiao *et al.*, 2008; Wang *et al.*, 2006, 2007). A significant correlation between the land accretion and the sediment input of YR was discerned through monitoring satellite images (Bi *et al.*, 2014; Chu *et al.*, 2005; Cui *et al.*, 2011), highlighting the critical role of the nurturing river system with respect to the health of the YRD.

However, most previous studies either focused on some specific features of the abandoned delta lobe with exceptional erosion rates (*e. g.* Ying *et al.*, 2007), or on the evolution of the active delta lobe (*e. g.* Wei *et al.*, 2013). There is limited information about the spatial comparison of the northern abandoned delta lobe and the active delta lobe of the YRD, as well as a comprehensive illumination of the dominant mechanisms of the evolution of the whole YRD since the deltaic river channel shifted in 1976. Moreover, the evolution of the subaqueous parts of the delta has not been systematically investigated. Furthermore, the sediment dispersion pattern, especially its temporal variation, has not been well understood within the source to sink framework. The general aim of this study is to establish an overall picture of the erosion and accretion pattern of the subaqueous YRD over the period of 1976 to 2004. The spatial and temporal variation of the general pattern was documented in detail, followed by discussion of the controlling factors, which may benefit the future management of the subaqueous YRD.

Study Area

The modern YRD is located southwest of the Bohai Sea, separating the Bohai Bay (BHB) in the west and Laizhou Bay (LZB) in the east (Figure 1a). The mean tidal range is 0.7 – 1.8 m along the coast of the YRD (Hu and Cao, 2003). An amphidromic point of M2 tide exists in the offshore area of the Shenxiangou (SXG) lobe with a minor tidal range of 0.4 m, and the tidal range gradually increases to 1.6–2.0 m towards the top of the BHB and LZB (Hu and Cao, 2003). The Qingshuigou (QSG) river mouth features a mixed semidiurnal tide, whereas the SXG river mouth is dominated by a mixed diurnal tide. The tidal currents flow in parallel with the coastline, with the flood current towards the south and ebb current towards the north. High tidal current is found at the offshore area of the abandoned SXG river mouth with a maximum rate of 1.3 m/s, and at the active QSG river mouth with a maximum rate of 1.87m/s (Pang and Jiang, 2003). Waves exhibit significant seasonality due to monsoon activity. The northerly waves in winter are much stronger than the southerly waves in summer. The stormy waves come from NE, with a maximum significant wave up to 5.2 m (Zang, 1996). The surface residual current flow southward at 20 – 30 cm/s in winter, whereas northward in summer (Zhang *et al.*, 1990).

Since the last diversion of the YR in 1855, a mega-delta, occupying a land area of more than 5,000 km^2, has been formed at the southwest of the BHS (Chu *et al.*, 2006), serving as a major sediment sink of the YR sediment. The annual sediment discharge amounts to 1.08 Gt/yr prior to 1980s (Milliman and Meade, 1983), and about 70% of the total sediment load was accumulated within 30 km around the river mouth (Wiseman *et al.*, 1986). The delta propagated rapidly into the BHS with land accretion rate of about 20 km^2/yr (Pang and Si, 1980). Since 1964, the deltaic river channel of the YR has shifted three times (Figure 1b). In 1964, an artificially diversion shifted the course from SXG channel westward to the DK channel, aiming to mitigate the risk of flooding in the delta plain. Then, in 1976, another man-made diversion shifted the river channel to the QSG channel, which continued to serve as the only distributary for the last 20 years. More recently, in 1996, a minor artificial shift redirected the river channel northward to the Qing 8 (Q8) river mouth, for the purpose of creating new land for the offshore oil fields in Gudong (Figure 1b).

METHODS

Since 1964, the Yellow River Hydraulic Committee has carried out profile surveys to document the bathymetric data along 36 fixed transects of the subaqueous delta lobe of the YR (Figure 1b). The profiles extend seaward with variable water depth, more than 15 m in the northern abandoned delta lobe, around 12 m in the active delta lobe, and less than 10 m in the west part of the LZB. The profile length varies from 20 to 60 km corresponding to different portions of the delta. Bathymetric data was collected approximately every 500 m along each transect, starting from ~2 m water depth. Distance between profiles ranges from 2 to 6 km. The bathometric data was converted to depths refering to the sea level datum of China after tidal correction. DH–13 digital echo sounder and UHF–547 microwave (GPS system for later period) were utilized to acquire the bathometric data and location data, respectively. The accuracy is about 10 cm for water depth and 2 m for position data. In this study, we collected bathometry data of 1976, 1980, 1985, 1990, 1996, and 2004 for analysis.

The daily sediment load and water discharge data from 1976 to 2004 was collected from the Lijin hydrological station, which is approximately 100 km upstream from the river mouth and is the nearest gauging station on the YR.

Data Analysis

The outer boundary of the calculation domain was determined as the–15 m, –12 m, and –9 m isobaths for the northern abandoned delta lobe, the active delta lobe and the LZB area, respectively, because they were the most commonly available water depth for the outer boundary. The –2 m water depth was considered as an acceptable inner boundary.

To facilitate the depth comparison, the original bathymetric data was interpolated at unified and fixed grid points, using the Kringing method. Then, the volume change was calculated by subtraction of the bathymetry of two years. Isobathic lines of–2 m, –5 m, –10 m, and –15m water depth were extracted, and their migration distance was measured in the transect direction u-

sing the ArcGIS 10. The maximum depth change along transects was determined with the aid of Global mapper 13, so is the average depth change along transects. The transect slope was defined as the depth difference between the −2 m isobaths and the corresponding outer boundary depth divided by the transect length.

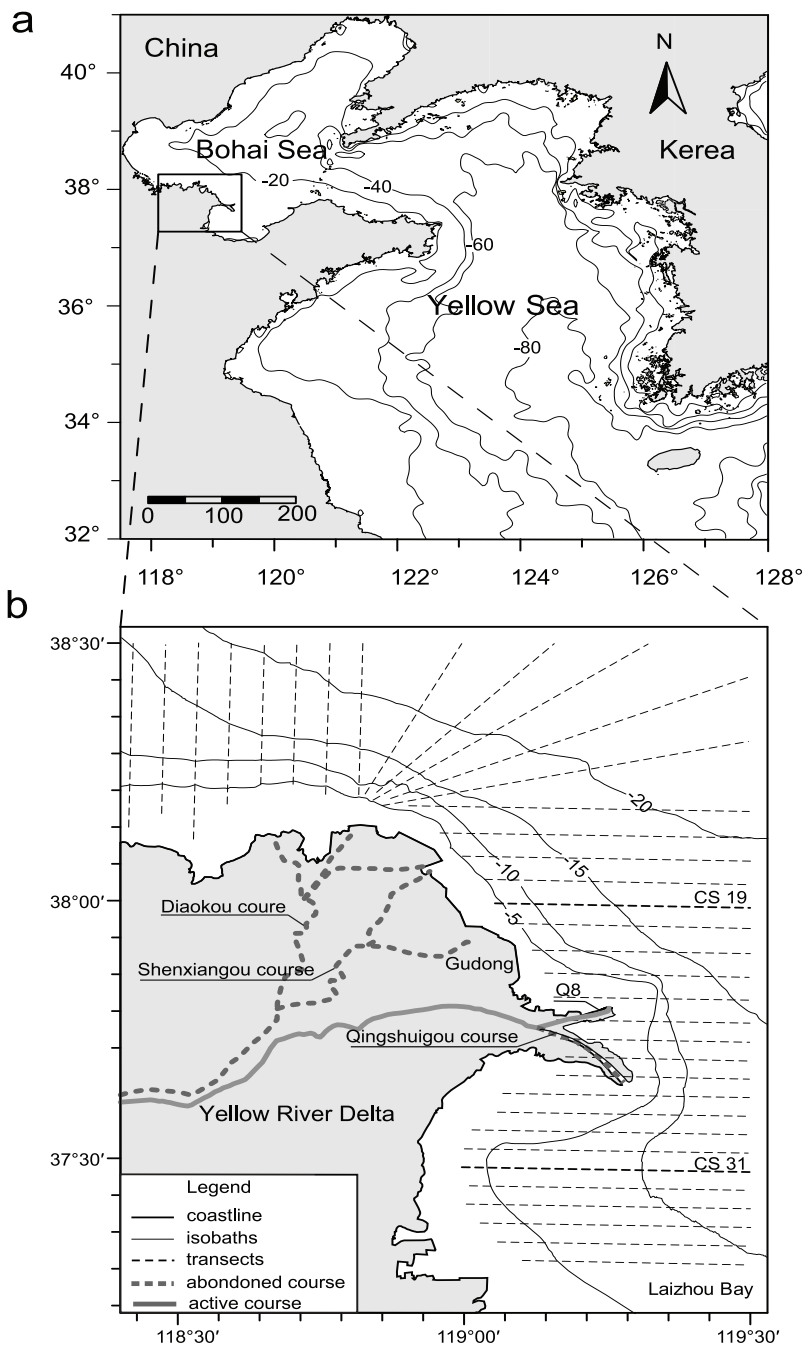

Figure 1. (a) Geographic settings of the Yellow River Delta (YRD). Water depth was acquired from ETOP1 data (http://www.ngdc.noaa.gov/mgg/global/global.html). (b) A close-up view of the YRD and locations of 36 transects off the YRD

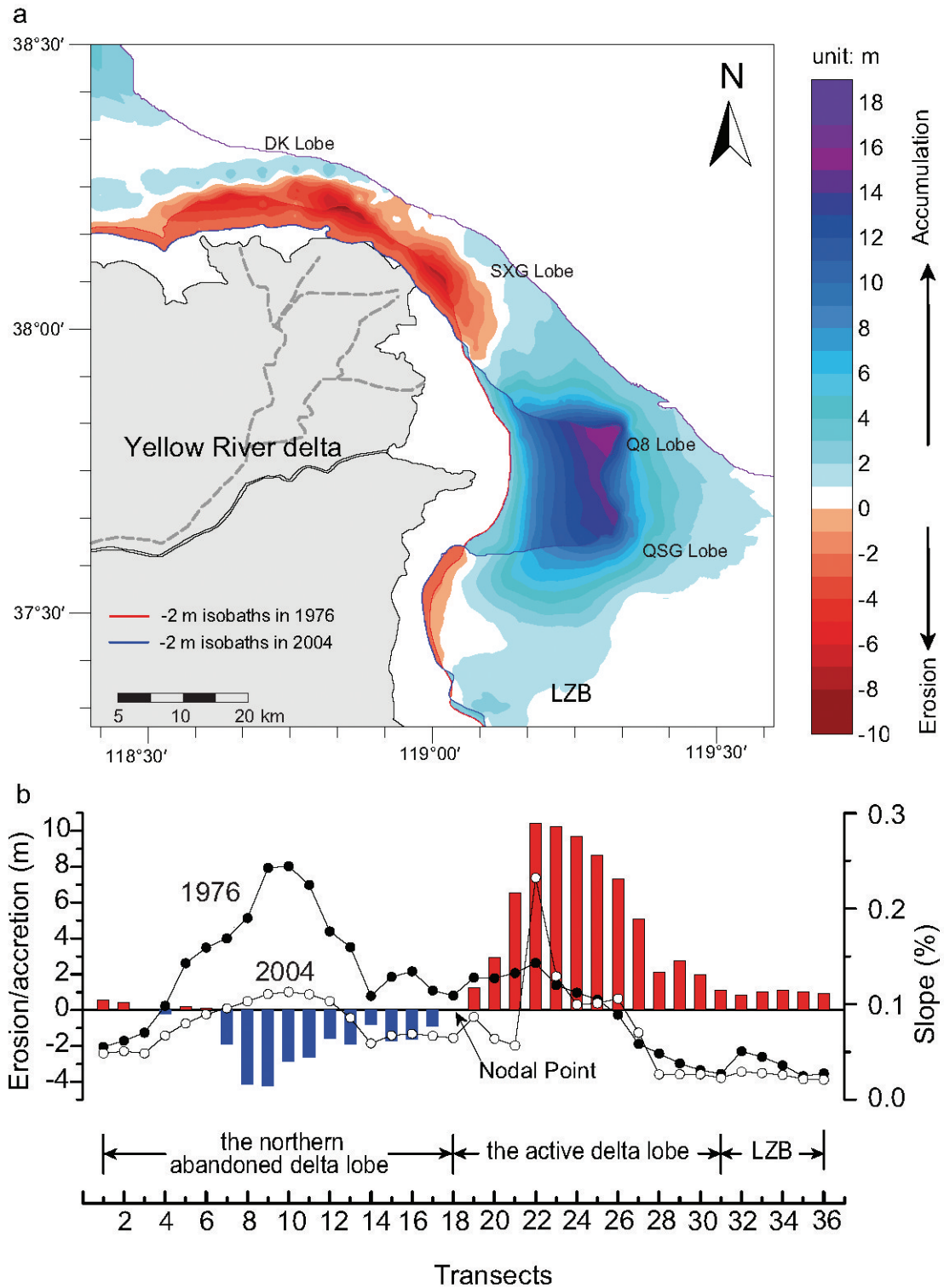

Figure 2. (a) Spatial variations of erosion and accretion of the Yellow river delta during 1976–2004. (b) Net erosion-accumulation thickness (bar plot) and slop variations along 36 transects (line with dot plot) during 1976–2004

RESULTS

The change in the bathymetry of the subaqueous delta lobe during 1976–2004 was analyzed to illustrate the temporal-spatial patterns of erosion and accumulation in the YRD.

Spatial Variations of Erosion and Accumulation in the YRD during 1976–2004

Erosion and Accumulation Thickness

The abandoned DK and SXG lobes experienced severe erosion (Figure 2a), forming three erosional centers off the abandoned DK and SXG river mouth. The maximum erosion thickness was approximately 7.5 m (Figure 2a). The erosion thickness gradually decreased seaward, away from the erosion centers, and turned into deposition at the offshore area with a maximum thickness of about 2.9 m (Figure 2a). A nodal point of erosion and accretion was found at transect CS 18 between the SXG and QSG lobes (Figure 2b). Further southward, the active delta lobe protruded eastward, forming the QSG lobe and the Q8 lobe, which was the active lobe after 1996. The maximum deposition thickness of the two delta lobes were approximately 15.1 m and 13.6 m, respectively, and decreased rapidly both in the littoral and seaward directions. It is worth noting that the deposition area extended both southward and northward in the offshore area, where the nearshore area was dominated with erosion regime (Figure 2a). Further southward, the LZB witnessed slight accumulation in the nearshore area with a maximum thickness of approximately 2.4 m, which was consistent with the aggradation area derived from the active delta lobe. The net erosion/accretion curve show the same pattern as described above.

Based on the spatial pattern of the erosion and accumulation in the YRD, the study area was divided into three regions (Figure 1a and Figure 2b). The northern abandoned delta lobe, between transect CS 1 and CS 18, consisted of the abandoned and heavily eroded DK and SXG lobes (Figure 2a). This region was characterized by severe erosion with a maximum net erosion thickness of approximately 4.2 m, although the western part showed slight net accretion (Figure 2b). The active delta lobe, between transect CS 19 and CS 31, comprised of the QSG and Q8 lobes (Figure 2a), which was dominant by significant progradation with a maximum net accumulation thickness of approximately 10.4 m (Figure 2b). The LZB between transect CS 32 to CS 36 witnessed slight accumulation with a maximum accumulation thickness of approximately 1.1 m (Figure 1 and Figure 2).

Slope

The slope curve showed mono-peak at the subaqueous abandoned delta lobe in 1976, with a maximum value of 2.5‰, decreasing to 0.55‰ at the westernmost abandoned delta and to 0.27‰ at the LZB. However, in 2004, the slope peaked at the active delta lobe with a maximum value of 2.3‰, corresponding to the maximum accretion area. The slope of the northern abandoned delta lobe decreased significantly with a maximum drop from 2.4‰ to 1.1‰, which agreed well with the erosion pattern. The northern margin of the active delta lobe saw significant slope decrease over the years whereas only subtle slope change occurred in the southern margin. The slope of the LZB decreased slightly from 0.5‰ to 0.3‰.

Isobaths migration

As a silt-muddy coast with very gentle subaqueous slopes, isobaths of the subaqueous YRD featured dramatic horizontal migration, which provided a sensitive indicator for the spatial patterns of the erosion and accretion of the YRD.

The −2 m and −5 m isobaths in the northern abandoned delta lobe retreated landward for approximately 6.9 km and 4.4 km, respectively (Figure 3a and 3b), indicating to the severe erosion in the nearshore area. As the isobaths varied from −2 m to −15 m, the landward retreat rate decreased significantly. Moreover, a seaward progradation tendency was detected by the increased number of accretion transects. The −15 m isobath was dominant by seaward accretion, although the magnitude was relatively small. As a whole, the variation of the isobaths in the northern abandoned delta lobe indicated that erosion occurred mainly at the shallow water area, while accretion occurred at the deep water area (Figure 3). As the active delta lobe protruded seaward, isobaths moved seaward dramatically. The progradation distance of the isobaths remained high seaward, while the range of accretion transects expanded laterally. The −2 m isobath at the south part of the active delta lobe retreat landward, which was quite different from the −5 and −10 m isobaths. The isobaths migration for the −2 m isobaths in the LZB was fairly small. The progradation distance increased seaward with a maximum value of 5.3 km for the −10 m isobaths.

Temporal Variationin Erosion and Accumulation of the Subaqueous YRD

To better investigate the temporal changes of this process, the erosion and accumulation of the subaqueous YRD with an interval of 4–8 years from 1976 were presented.

1976– 1980

During the period of 1976–1980, the abandoned delta lobe suffered rapid erosion with a maximum erosion rate of 1.5 m/a (Figure 4). Both the deep and shallow water areas showed erosion conditions, with three erosion centers developed at the nearshore area. The active delta lobe witnessed rapid deposition, 1.7 m/a as a maximum rate, constructing a south-north narrow accumulation belt. The accumulation rate decreased seaward, and turned into erosion at the outer periphery. The LZB was eroded slightly at the nearshore area, and accumulated slightly at deeper area (Figure 4).

The transect-averaged erosion rate (net erosion rate) of the northern abandoned delta lobe was the highest among all periods, with a maximum erosion rate of 0.8 m/a at transect CS 9 (Figure 5). The net erosion rate decreased laterally away from the erosion center. The active delta lobe was characterized by rapid aggradation, with a maximum transect-averaged accumulation rate (net accumulation rate) of 0.9 m/a. Moreover, the accumulation was mainly on the northern part of the active delta lobe, without prominent depocenters. Meanwhile, the southern part of the active delta lobe and the LZB had no significant depth change. The slope of the subaqueous delta lobe with high values at intensively eroded area decreased dramatically from 2.4‰ to 2.0‰, and the magnitude of the slope change gradually reduced away from the erosion centers. The slope of the active delta lobe increased considerably from 1.0‰ to 2.0‰, with formation of a platform-type peak (Figure 5).

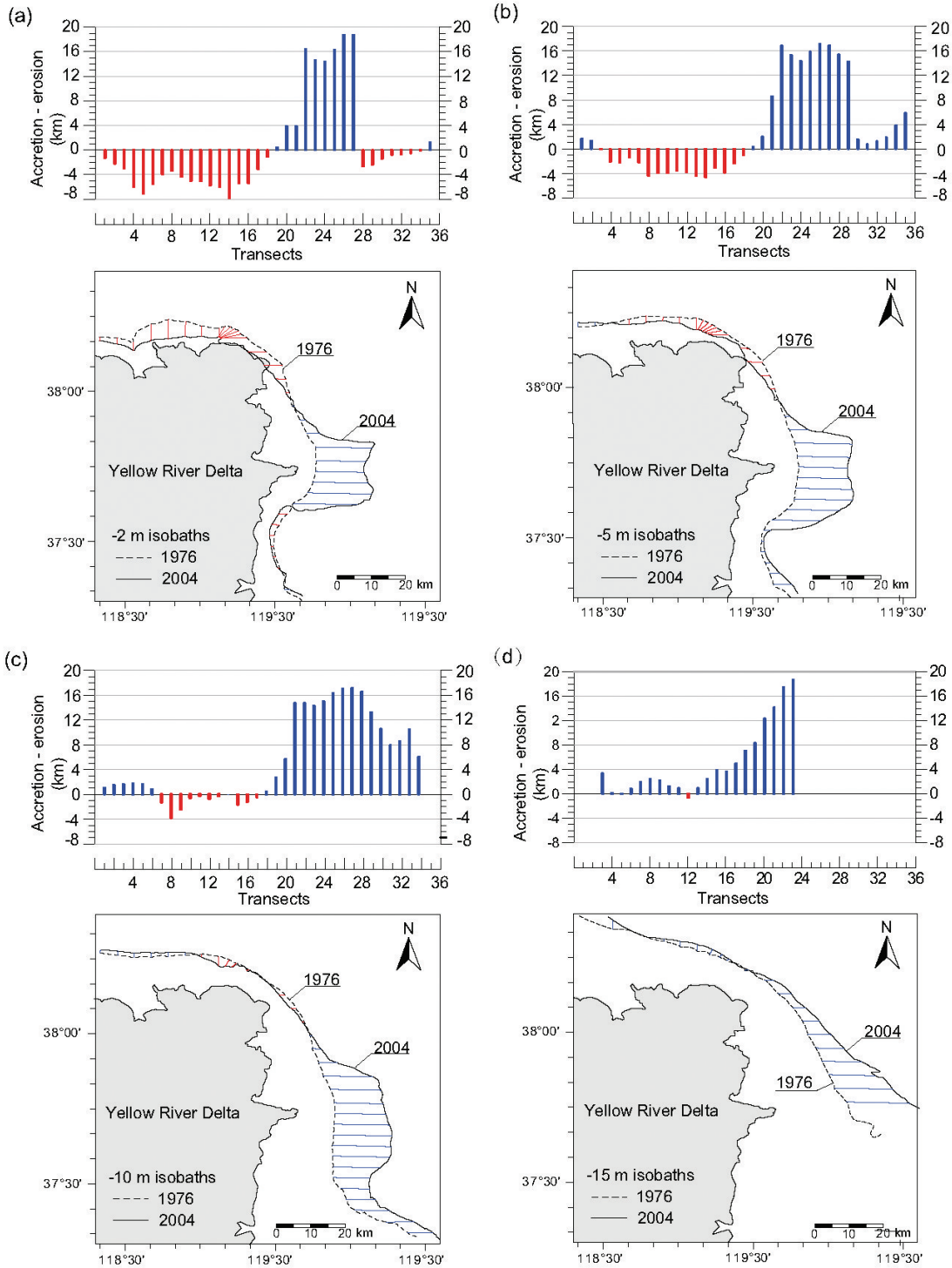

Figure 3. Spatial variations of isobaths during 1976 −2004. (a), (b), (c) and (d) represent −2 m, −5 m, −10 m and −15 m isobaths displacement, respectively (note: red bars indicate erosion, and blue bars indicate accretion). Sketch map showed how to compute the distance of isobaths migration during the period 1976 to 2004

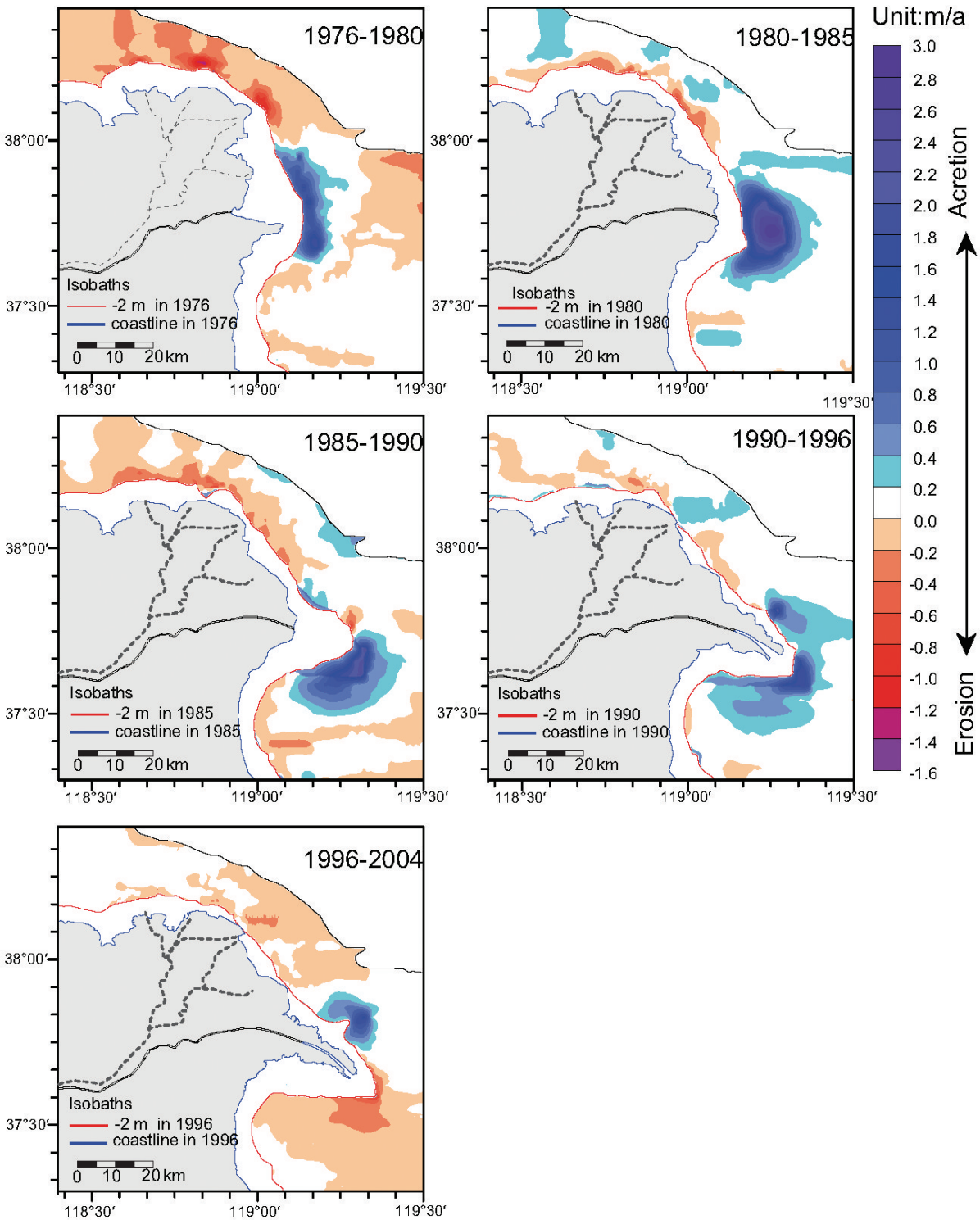

Figure 4. Temporal variations of erosion and accumulation pattern of the YRD

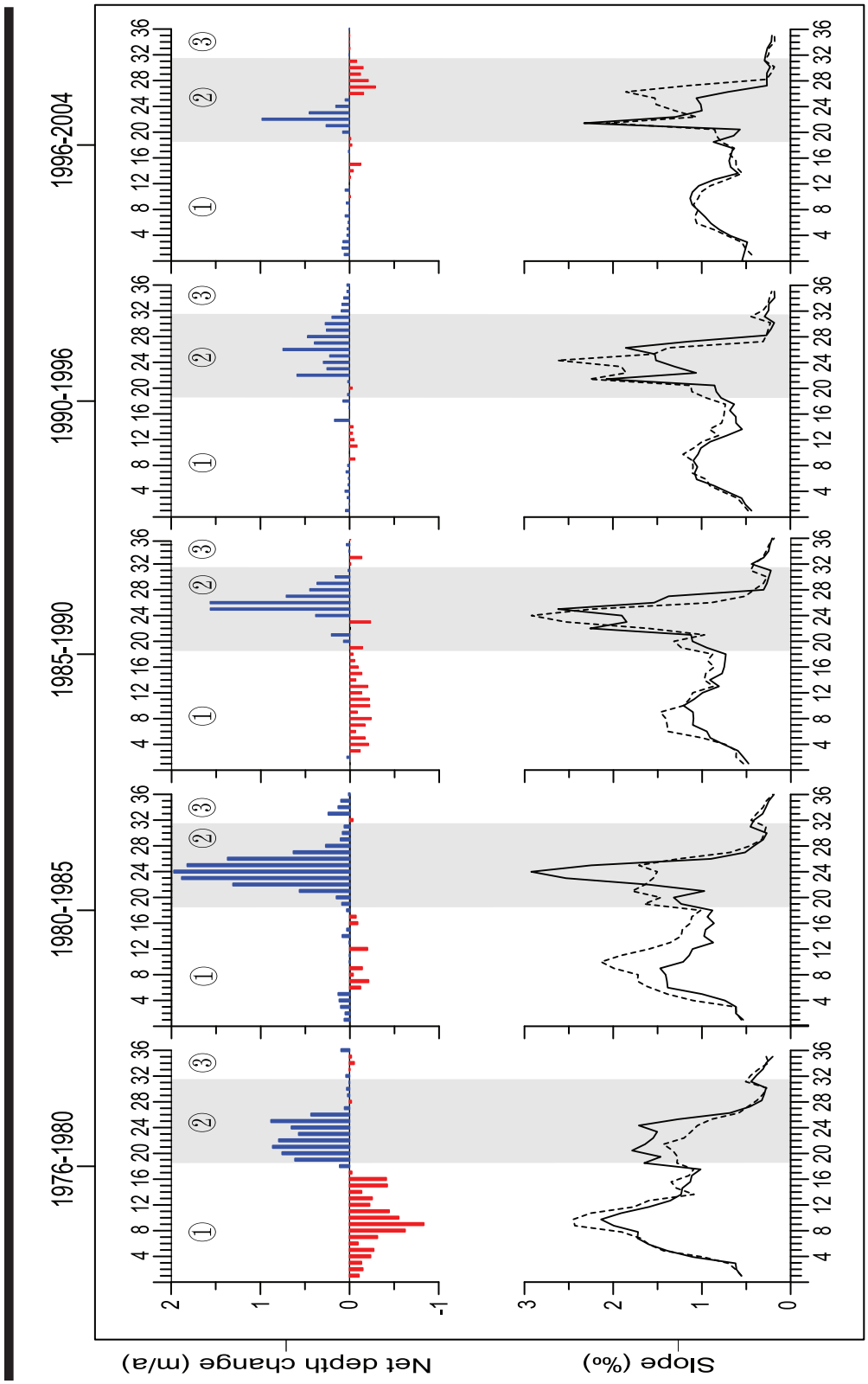

Figure 5. Transect-averaged net depth change along transects cs1- cs36 for 1976-1980, 1980-1985, 1985-1990, 1990-1996, and 1996-2004, respectively (bar plot). Variation of slope along the 36 transects for periods mentioned above, with the dashed line for the starting year, and the solid line for the ending year (line plot). Number ①,② and ③ representing the northern abandoned delta lobe, the active delta lobe (in shadow region) and the LZB, respectively

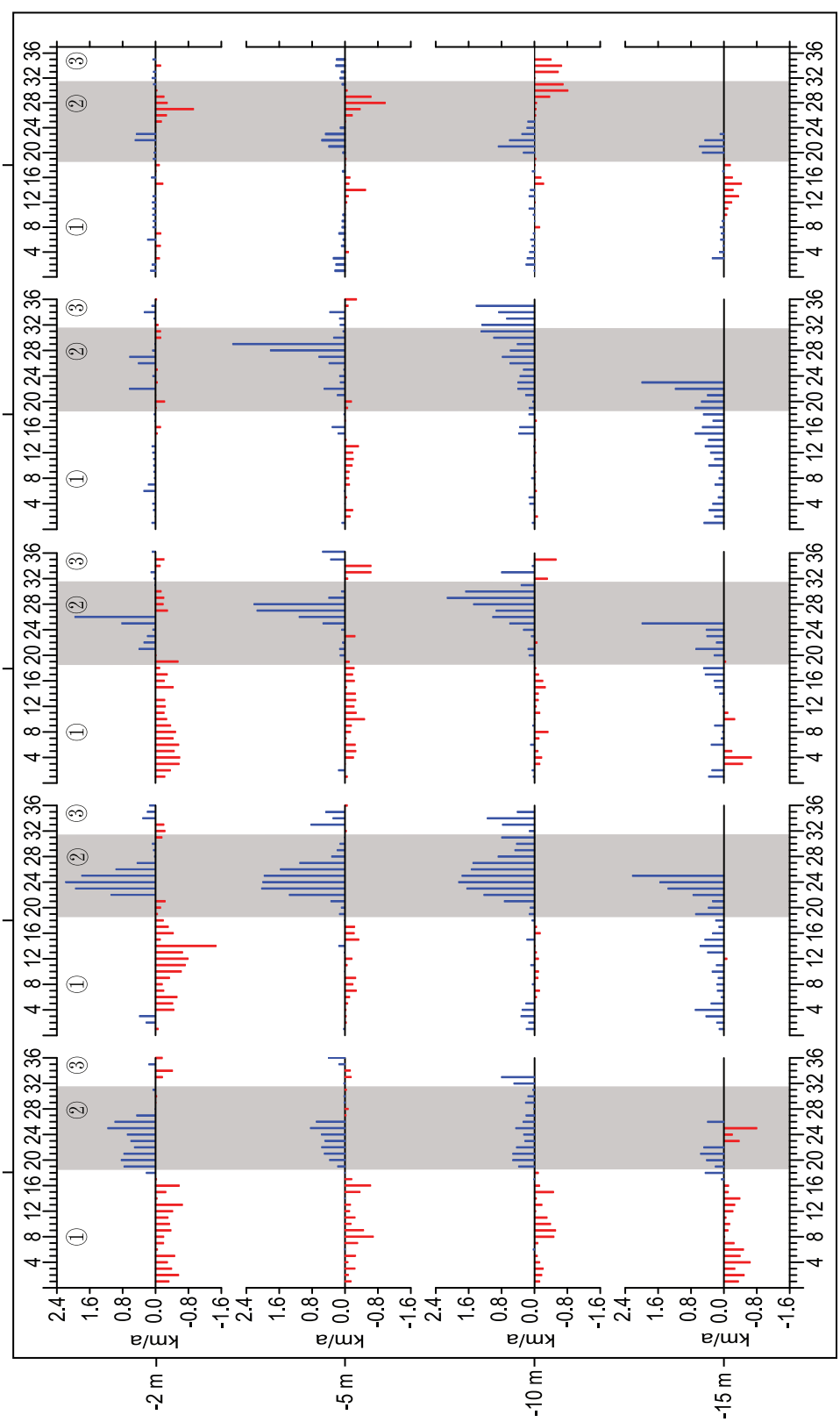

Figure 6. Landward/seaward change of the -2, -5 m, -10 m, and -15 m isobaths for period of 1976-1980, 1980-1985, 1985-1990, 1990-1996, and 1996-2004, respectively. Positive value indicates seaward propagation, while negative value indicates landward retreat. Numbers of ①,② and ③ are consistent with those in figure 5

Landward retreat of isobaths was witnessed in both the shallow and deepwater areas of the northern abandoned delta lobe with a maximum rate of 0.5–0.7 km/a (Figure 6). Among all periods, the −2 m isobath of the active delta lobe displayed the widest range of seaward accretion. The maximum progradation rate decreased seaward notably from 1.2 km/a to 0.5 km/a, while erosion occurred at the −15 m isobath of the active delta lobe. Meanwhile, the range of progradation expanded obviously at the −10 m isobaths. The LZB was featured with a landward retreat at the −2 m and −5 m isobaths, but a seaward accretion tendency at the −10 m isobath, with a maximum rate of 0.80 km/a (Figure 6).

1980–1985

The erosion area in the northern abandoned deltalobe shrank to the shallow water area with a reduced maximum erosion rate of 0.7 m/a, while accumulation occurred offshore with a maximum rate of 0.4 m/a (Figure 4). The active delta lobe formed a driplike accumulation area eastward with a maximum accumulation rate of 2.7 m/a, which was by far the largest among all periods. The LZB was dominant by slight accumulation (Figure 4).

The net depth changeof the northern abandoned delta lobe decreased remarkably, with a maximum erosion rate of 0.2 m/a and a maximum accumulation rate of 0.1 m/a (Figure 5). A prominent and laterally symmetrical depocenter developed at the active delta lobe, with a maximum accumulation rate of 2.0 m/a, which is the largest among all periods. The LZB area saw slight accumulation with a maximum rate of 0.2 m/a. The slope of the abandoned delta lobe witnessed a major decrease from approximately 2.1‰ to 1.2‰, occurring in erosion centers (Figure 5). The slope of the active delta lobe jumped from 1.5‰ to 2.9‰, forming a sharp peak at transect CS 24. Meanwhile, the slope reduced notably at the northern part of the active delta lobe from 1.8‰ to 1.0‰, whereas remained relatively stable at the southern part. The slope of the LZB witnessed a minor decrease (Figure 5).

The isobaths variation of the northern abandoned deltalobe showed different pattern from the previous period with landward retreat in the nearshore area and seaward progradation in the offshore area. The maximum landward retreat rate of the −2 m isobath was 1.47 km/a, but decreased to 0.34 km/a and 0.14 km/a for the −5 m and −10 m isobaths, respectively. The −15 m isobath turned into seaward accretion with a maximum rate of 0.68 km/a (Figure 6). The active delta lobe area accreted rapidly with a maximum accretion rate of 2.19 km/a for the −2 m isobath (Figure 6). The progradation rate generally remained its intensity seaward, with a maximum rate of 1.85–2.20 km/a for the −5 m, −10 m, and −15 m isobaths. The accretion range in the shallow water area was narrower than the previous period as indicated by the erosion and accretion of the −2 m isobaths, and it also expanded in the deep water area. The LZB was dominated with accretion with a maximum rate of 1.15 km/a for the −15 isobath, and erosion was limited to the south of the active delta lobe (Figure 6).

1985–1990

The general pattern of the northern abandoned deltalobe during 1985–1990 was the same as that during 1980–1985. However, the erosion area with a maximum rate of 0.6 m/a expanded southeastward and seaward. The deposition center of the active delta lobe migrated southeastward with a maximum accumulation rate of 1.1m/a, leaving the north side of the active delta lobe suffering erosion with a maximum rate of 0.8 m/a (Figure 4). The nearshore zone of the LZB was mainly in erosion regime with a maximum rate of 0.3 m/a, while the offshore area mainly showed accumulation regime with a maximum rate of 0.4 m/a (Figure 4).

The net depth change of the northern abandoned delta lobe was dominantby erosion with a maximum rate of 0.2 m/a in erosion center (Figure 5). The maximum net accumulation rate of the active delta lobe reduced to 1.6 m/a. Moreover, the accumulation rate showed asymmetric pattern, in which the southern margin displayed gradual reduction of the accumulation rate, while the northern margin showed abrupt occurrence of erosion. The net depth change of the LZB showed erosion at the north part and accumulation at the southern part, all with small magnitude. The slope of the abandoned delta lobe continued to decrease, from 1.4‰ to 0.9‰ at the DK lobe. The slope decreased from 2.9‰ to 1.9‰ at the former depocenter, and increased from 0.5‰ to 1.4‰ at the southern part of the active delta lobe. The slope of the LZB area showed no significant variation.

The general pattern of the isobaths variation in the northern abandoned deltalobe remained the same as that during 1980–1985, although the maximum erosion rate reduced to 0.58 km/a (Figure 6). The accretion range of the active delta lobe was smaller than the previous periods, with a slightly reduced maximum rate of 1.94 km/a. The accretion range expanded seaward, and the accretion rate increased southward, indicating that the deposition center shifted southeastward. The LZB witnessed both landward and seaward isobath shift with no obvious tendency (Figure 6).

1990–1996

The northern abandoned delta lobe remained as erosion in the shallow water area and accumulation in the deep water area. However, the erosion zone was much smaller than the previous periods, and the maximum erosion rate reduced to 0.4 m/a. Two depocenters developed in the active delta lobe, with the major one at the QSG lobe and the other one at the Q8 lobe with a maximum aggradation rate of 1.7 m/a and 1.6 m/a, respectively. The LZB was dominated with slight accumulation (Figure 4).

The net depth change of the northern abandoned deltalobe was less than the previous periods (Figure 5). Erosion shrank to the northeastern part of the YRD with a maximum rate of 0.1 m/a, and turned into accumulation laterally with a maximum rate of 0.2 m/a. The net accumulation rate of the active delta lobe reduced significantly with a maximum rate of 0.6 m/a and 0.7 m/a for the Q8 and QSG depocenters, respectively. The southern part of the QSG lobe and the LZB area showed slight reduction of accumulation rate, whereas the north of the Q8 river mouth exhibited abrupt termination of accumulation. The slope was almost unchanged for the western part of the northern abandoned delta lobe, but decreased from 0.9‰ to 0.5‰ at the southeastern part (Figure 5). The slope variation pattern of the active delta lobe was similar with the previous period, with two slope peaks formed at QSG and Q8 lobe, both lower than their previous values during the period of 1985–1990. The slope of the LZB decreased from 0.4‰ to 0.3‰ at the north margin, and almost unchanged southward (Figure 5).

The general pattern of the isobaths variation in the northern abandoned deltalobe remained the same as that during 1985–1990, with retreat rate of isobaths in the nearshore area reducing

to 0.21 km/a and the accretion rate in the offshore area increasing to 0.53 km/a. The seaward progradation rate of isobaths in the active delta lobe increased southward with a maximum value of 2.73 km/a for the −5 m isobath. The −10 m isobath of the LZB saw rapid seaward progradation with a maximum rate of 1.42 km/a, whereas the −2 m and −5 m isobaths varied slightly (Figure 6).

1996–2004

The western part of the northern abandoned deltalobe was in a slight accumulation regime with a maximum rate of 0.3 m/a, while the eastern part was dominated by erosion regime with a maximum rate of 0.4 m/a. The middle part of the northern abandoned delta lobe was eroded nearshore and accumulated offshore. The depocenter at the nearshore area of the Q8 lobe continued to develop with a maximum accumulation rate of 1.3 m/a. The QSG lobe, however, shifted from a depocenter during the previous periods to an erosion center with a maximum rate of 0.8 m/a. The erosion area extended southeastward to the offshore area of the LZB, where slight accumulation occurred in the shallow water area (Figure 4).

The western part of the northern abandoned deltalobe accreted seaward with a maximum rate of 0.1 m/a, while the eastern part presented erosion with a maximum rate of 0.1 m/a (Figure 5). The active Q8 river mouth witnessed rapid progradation with a maximum net accumulation rate of 1.0 m/a, whereas the abandoned QSG river mouth experienced severe erosion with a maximum rate of 0.3 m/a. The net depth change of the LZB was negligible. The slope of the northern abandoned delta lobe varied slightly, which agreed well with the depth change (Figure 5). The slope of the Q8 river mouth increased from 2.1‰ to 2.3‰, while the slope of the QSG river mouth dropped dramatically from 1.9‰ to 0.7‰. The slope of the LZB area was almost unchanged.

The migration of isobaths in the north abandoned delta lobe varied slightly. The western abandoned delta lobe was dominant with accretion regime, whereas the eastern part displayed a landward retreat regime with a maximum rate of 0.42 km/a, occurring at the −15 m isobath (Figure 6). Isobaths in the active Q8 lobe migrated seaward with a maximum rate of 0.50 km/a, 0.56 km/a and 0.88 km/a for the −2 m, −5 m and −10 m isobaths, respectively, which were the lowest values since 1980. Meanwhile, isobaths of the QSG river mouth retreated landward rapidly with a maximum rate of 0.98 km/a, occurring at the −5 m isobath. The retreat center moved southward, as isobaths vary from −2 m to −10 m isobaths. The −10 m isobaths of the LZB experienced the fastest landward retreat among all periods, whereas the −2 m and −5 m isobaths shifted seaward slightly, indicating a slight accumulation occurred at shallow water area (Figure 6).

DISCUSSION

Process and Mechanism of Erosion and Accumulation of the Northern Abandoned Delta Lobe

The evolution of the northern abandoned delta lobe can be divided into three stages. Stage I, from 1976–1980, had the highest erosion rate among all periods, and both the nearshore and the offshore areas exhibited erosion (Figure 5 and Figure 6). During stage II, from 1980 to 1996, the mean erosion rate gradually reduced, and the erosion area expanded to the coastal zones. Moreover, erosion in the nearshore area and accumulation in the offshore area occurred simultaneously as indicated by the isobaths variation (Figure 6), resulting in a pronounced decrease in the slope of the subaqueous delta lobe (Figure 5). Stage III presented even lower erosion and accumulation rates with a gentle and slightly varied slope, which suggested a relatively equilibrium state of regional sediment dynamics, although the eastern and western part of the northern abandoned delta lobe showed different erosion and accumulation conditions (Figure 4, 5, and 6).

It is hardly surprising that rapid erosion occurred at the northern abandoned delta lobe after the cutoff of sediment supply in 1976, given the low sediment strengths created by rapid deposition in the preceding period, the steep bottom slope and the prevailing wave directions (Prior*et al.*, 1989). High turbidity zones at the coastal area of the northern abandoned YRD have been identified by field observation and satellite images (Yang, *et al.*, 2011), which directly resulted from the re-suspension process driven mainly by wave process, and partially by tidal currents (Chen *et al.*, 2005; Wang *et al.*, 2006; Yang, *et al.*, 2011). The suspended sediment was then transported outward by the combined flow of waves and tidal currents especially during the winter seasons when the northerly storm-generated waves frequently strike the BHS. Moreover, the seabed instability phenomena such as wide shallow gullies, collapse depression, fluidization-induced landslides (Prior *et al.*, 1986; Yang *et al.*, 1994), offered valuable insight into the mass movement related erosion process occurring at the seabed, which was triggered not only by wave-current induced bottom shear stress but also by the wave-induced strength inhomogeneity of the seabed sediments (Liu *et al.*, 2013).

During stage II, the erosion rate of the nearshore area has been slowed down, which can be attributed to the gentler subaqueous slope (Figure 5) and the enhanced sediment resilience under wave action (Jia *et al.*, 2011). Moreover, the offshore area witnessed accumulation while the nearshore area saw erosion (Figure 4), which can be explained by down-slope sediment transport process. Since wave energy was convergent in the nearshore area, high-turbidity zone was formed due to active re-suspension of the bottom sediment under high wave-induced bed shear stress. The fine suspended sediment was then entrained in the fluid mud layer, transported down-slope by gravity, and deposited at the offshore area, which was supported by the observation of down-slope sediment composition on seabed and in the water column (Wang *et al.*, 2006). This down-slope transport process effectively reduced the slope of the subaqueous delta lobe (Figure 5), and accelerated the evolution towards an equilibrium profile.

During stage III, the northern abandoned delta lobe was in equilibrium state. However, the erosion in the offshore area off the SXG lobe had experienced renaissance, which might be related to the decline of the down-slope sediment transport, such as the silt flow, due to the gentler slope and the enhancement of the erosion resistance of the seabed sediment. Consequently, the resuspended sediment was less transported along the slope and deposited at the offshore area but mainly transported alongshore away from the abandoned delta lobe by the currents, resulting in a regional loss of sediments. Moreover, after 1996, the river-laden sediment discharge exhibited significant decrease (Figure 7a) and mainly deposited at the nearshore areas around the Q8 river mouth (Figure 4e), which may cause a significant reduction of the northward sediment transport in the offshore area.

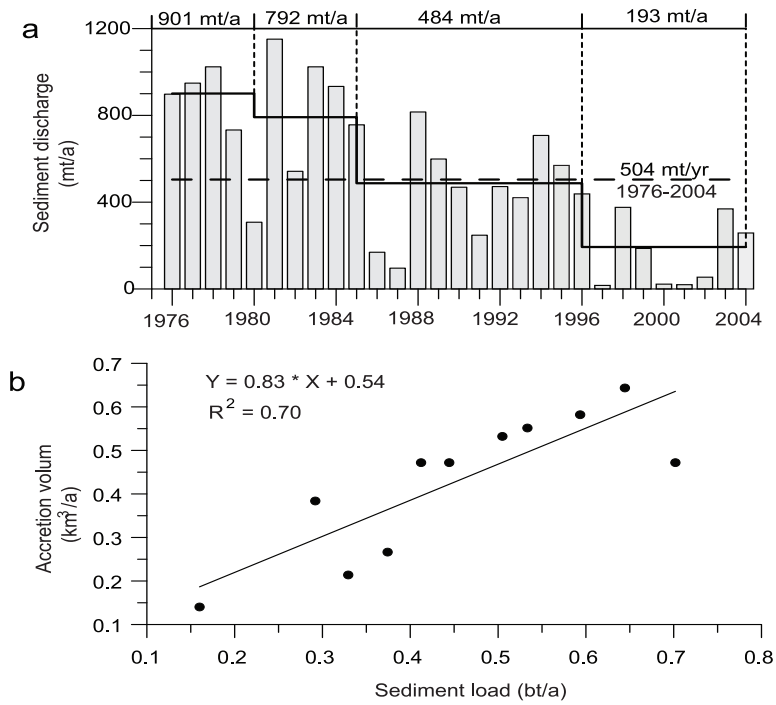

Figure 7. (a) Variations in annual sediment load at Lijin hydrologic station (bar plot). (b) Relationship between the annual sediment load at Lijin station and the annual volume change of the active subaqueous delta lobe during the period of 1980–1999 (data was from Zuosheng Yang (personal communication))

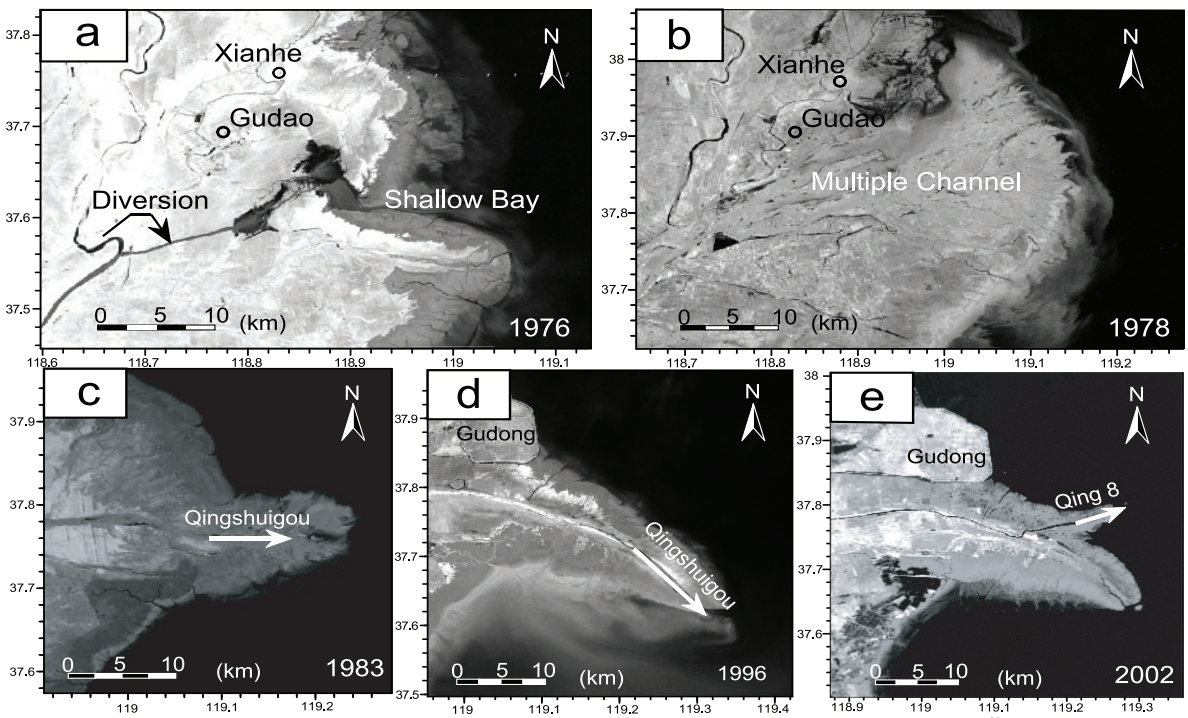

Figure 8. Evolutions of the deltaic river channel of the Yellow River and the YRD presented by the Landsat images (http://glovis.usgs.gov/). (a) The Yellow River flowed into a shallow bay when the river just migrated from the DK course to the QSG course in 1976, (b) multiple river channels and overflows, (c) river channel extending eastward, (d) river channel turning southeastward, and (e) river channel shifting northeastward

Process and Mechanism of Erosion andAccumulation of the Active Delta Lobe

The evolution of the active delta lobe can be divided into four stages. Stage I was from 1976 to 1980 when a narrow deposition area formed along shore with multi-depocenter. The most obvious feature of stage II, from 1980 to 1985, was its rapid progradation rate, formed a projected deposition body eastward with a single depocenter. During stage III from 1985 to 1996, the progradation rate went down, and the depocenter shifted towards the southeast of the QSG river mouth. The new deposition area formed at the Q8 river mouth marked a new stage, from 1996 to 2004, when the QSG river mouth underwent severe erosion. The dominant factors controlling the erosion and accumulation of the active delta lobe are as follows:

River Sediment Load

Delta dynamics is mainly a function of sediment input from the rivers (Chu *et al*., 2006; Cui and Li, 2011). The erosion and accumulation of the active delta lobe was closely related to the sediment load at Lijin station (Figure 7). The annual sediment load at station Lijin during 1976–2004 was 504 Mt/yr (Figure 7a), about two thirds of which were accumulated at the subaqueous delta lobe (Chen *et al*., 1998). However, the sediment discharge had experienced stepwise decrease from 901 Mt/yr in the period of 1976–1980 by 12%, 39%, and 60% for 1980–1985, 1985–1996, and 1996–2004 (Figure 7a), respectively, primarily due to extensive human intervention and climate change (Wang *et al*., 2007a; Wang *et al*., 2010). As a result, the accumulation rate, as well as the isobaths progradation rate of the active delta lobe generally tended to be declining after 1985 (Figure 5 and Figure 6). Additionally, since the initiation of the Water-Sediment Regulation Scheme (WSRS) in 2002, the grain size of the sediment load has increased significantly from 17.2μm to 25.5μm with the resultant setting velocity increasing more than twice that before WSRS (Bi *et al*., 2014; Wang *et al*., 2011). Consequently, more sediment was deposited at the neareshore area, formed a nearshore aggradation area much smaller than the previous period (Figure 4).

Channel Geometry

From 1976 to 2004, the QSG distributary had evolved through four channel patterns. During 1976–1980, the receiving estuary remained as a shallow embayment (Figure 8A), and the QSG channel was in its incipient stage, with the sediment-laden overflow flooding on the precedent delta plain during flooding season. The river-laden sediment was accumulated at the flooding plain, and filled up the shallow embayment area (Figure 8B). Thus, the deposition at the subaqueous delta lobe was much less than the sediment load at station Lijin, and the accumulation rate was less than the following period (Figure 5), despite the higher sediment load at this period. Moreover, since the river water was conducted through multi-channels (Figure 8B), the discharge would be divided up into several moderate flows with enlarged hydraulic radius and reduced velocity (Syvitski *et al*., 2005). Therefore, with the reduced transport capacity, more suspended sediment was captured near the river mouth as a narrow belt (Figure 4), and the isobaths progradation distance exhibited notable seaward decrease (Figure 5). Furthermore, the frequent distributary channel migration would account for the wide lateral range of the accretion area and the multi-depocenters (Figure 4, 5 and 6).

After the flood season of 1980, the multi-channels of the Yellow River evolved into a single channel projecting eastward (Figure 8C), which would enhance the sediment delivery to the subaqueous delta lobe by regulating the flow within the main channel. Consequently, the subaqueous delta lobe prograded eastward rapidly with a thick depocenter developed, whereas the accretion range shrank obviously (Figure 5 and Figure 6). During 1985–1996, the river extended southeastward (Figure 8D) under the combined effects of the Coriolis force and the hydrodynamics (*e. g.*, tidal currents, circulation and waves). As the river mouth prograded further away from the neighboring coast, southeastward sediment transportation was enhanced, and more sediment was deposited in the deep area of the LZB (Figure 4, 5, and 6). Meanwhile, the northern flank of the river mouth was in erosion regime, accompanied by significant slope drop (Figure 5). The river channel shifted to the Q8 river mouth after an artificial diversion in 1996 (Figure 8E), caused the accretion around the new river mouth and severe erosion around the abandoned QSG river mouth (Figure 4e).

Hydrodynamics

Once sediment discharged into the coastal area, its movement would be influenced by ocean dynamics. The topography-enhanced tidal current off the spit-like delta was the dominant natural force acting on the sediment dispersion pattern of the YRD (Li *et al*., 1998; Pelling *et al*., 2013). The seaward-flowing momentum of the YR was retarded by the isobaths-parallel tidal current, and was transported southward by the flood current and northward by the ebb current, contributing to the aggradation of the subaqueous delta lobe (Figure 4).

Another important factor should be ascribed to the shear front. Due to the trapping effect of the shear front, most of the river-laden sediment, whether carried by river plumes or hyperpycnals, was retained and deposited in the shallow area, accounting for the rapid accumulation of the subaqueous slope (Wang *et al*., 2007). The lateral sediment dispersion was effectively maintained within the deep water areas by the combined effect of tidal shear front and the isobath-parallel tidal currents (Bi, *et al*., 2010). Consequently, the coastal areas around the active delta lobe were in erosion state (Figure 2). The tidal shear front had been generated, strengthened, and pushed seaward by the prominent subaqueous slope of the river mouth (Qiao *et al*., 2008). Thus its barrier effect will continuously affect the sediment dynamics of the YRD.

Strong storm waves are prevailing in winter at the YRD with a maximum significant wave height of 5.2 m (Zang, 1996), working as destructiveforces with significant resuspension and erosion effect of the seabed. The southward shift of the subaqueous depocenters (Figure 4, 5, and 6) was partly caused by the southward sediment transport driven by winter waves and wind-driven currents (Yang *et al*., 2011). Since 1976, the projection of the YRD has enhanced the tide amplitude by 20 cm according to the tide-gauge records at Yangjiaogou Station (Zhang and Wang, 2000) as well as model simulations (Pelling *et al*., 2013), which was speculated to reinforce the storm surges and wave set-ups (Kim *et al*., 2008). Slope failures were observed at the subaqueous delta lobe (Prior *et al*., 1989), which facilitated

the sediment escaping from the deltaic region by down-slope sediment transport. Thus, the erosion of the storm waves and surges may have been increasingly important in the evolution of the YRD.

Process and Mechanism of Erosion and Accretion of the LZB

During the period of 1976–2004, the LZB witnessed slight accumulation with the subaqueous slope decreasing slightly and the isobaths shifting seaward. Before 1996, the seaward progradation of isobaths was enhanced towards the −10 m isobaths (Figure 6), whereas, after 1996, the erosion area of the abandoned QSG lobe extending southeastward to the offshore area of LZB and the −10 m isobaths witnessed significant landward retreat (Figure 4 and Figure 6).

The erosion and accretion pattern of the LZB area was closely associated with the sediment dispersion pattern off the active delta lobe. High suspended sediment concentration (SSC) was observed extending eastward or southeastward off the river mouth to the central part of LZB (Bi *et al.*, 2010; Qiao *et al.*, 2010; Yang *et al.*, 2011), which indicated that the deposition at the offshore area of LZB was mainly from the prevailing southward sediment transportation off the active river mouth. As the active delta lobe progradated southeastward, more sediment was deposited at the offshore area of LZB. After the diversion of the YR in 1996, the riverine sediment mainly discharged northeastward, and rapidly deposited at the nearshore area (Bi *et al.*, 2014; Wang *et al.*, 2011), which would cause less sediment transported southward into the LZB. Consequently, the offshore area of LZB shifted from accumulation into erosion. Thus, the offshore area of the LZB was more actively responding to the sediment dispersion of the active delta lobe than the nearshore area, which can be best explained by the shear front effect off the active delta lobe. The existence of tidal shear fronts in the southern shallow water areas of the active delta lobe, combined with the isobath-parallel tidal current prevent the riverine sediment from reaching the nearshore area of LZB and resulted in the offshore deposition. However, the LZB area has experienced only slightly accumulation, which seems inconsistent with the long-term southward sediment transportation. It is believed that the LZB only serve as a temporal sediment sink in summer, and might be a sediment source in winter due to the powerful effect of winter storms (Yang *et al.*, 2011). Consequently, the LZB acted as a sediment passage for the outward sediment transport, and the massive sediment did not deposited here in the long run (Hu *et al.*, 2006).

Riverine sediment supply is critical for the survival of deltas. The cutoff of sediment supply had caused severe coastal erosion on the northern abandoned delta lobe. However, the erosion rate has been gradually slowing down due to the decrease of the subaqueous slope and the increase of the geotechnical strength of the sediment (Jia *et al.*, 2011, Ying *et al.*, 2007). Thus, the northern abandoned delta lobe will evolve towards a relatively balanced state with equilibrium profiles. After the initiation of WSRS, the annual sediment discharge of the YR increased slightly from 0.15 Gt (2003–2011) to 0.17 Gt/yr (2003–2011), which was greater than 50 Mt, the calculated critical sediment discharge for maintaining the dynamic equilibrium between erosion and accretion in the active delta lobe (Bi *et al.*, 2014). In addition to the increase of sediment discharge, the sediment grain size increased because the flushed river-bed sediment by the artificial flood became a major sediment source. The coarsening of the particle size of the suspended sediment after initiation of the WSRS also favored nearshore sediment deposition (Bi *et al.*, 2014; Wang, *et al.*, 2010, 2011). However, recent study indicates that the erosion rate of the river bed is decreasing gradually because the river bed is becoming more resistant to erosion. The grain size of the sediment decreases gradually after 2012 (unpublished data). Therefore, we speculate the progradation rate will decrease for the active YRD in the coming years.

CONCLUSIONS

The evolution of the subaqueous YRD presented significant spatial and temporal variability during 1976–2004. Three regions were delineated based on the spatial pattern of the erosion and accumulation in the YRD, *e. g.* the northern abandoned delta lobe, the active delta lobe and the LZB, which was characterized by server erosion, significant progradation and slight accumulation, respectively.

The evolution of the northern abandoned delta lobe can be divided into three stages: rapid erosion (1976–1980), nearshore-erosion and offshore-accumulation (1980–1996), and adjustment (1996–2004). The erosion rate of the northern abandoned delta lobe gradually reduced over time, and reached a relatively balanced state. The evolution of the active delta lobe experienced four-stage variation pattern. During 1976–1980, a narrow deposition area was formed along shore of the active delta lobe with multi-depocenter. It changed to an eastward projected deposition body with single depocenter and increased accumulation rate during the period of 1980–1985. The depocenter shifted towards the southeast of the QSG river mouth with a slow-down accumulation rate from 1985 to 1996, and it shifted again to Q8 river mouth with a narrowed accumulation range during 1996–2004, when the QSG river mouth underwent severe erosion. The evolution of the LZB witnessed two-stage variation pattern. Before 1996, the LZB was dominant by slight accumulation, especially at the offshore area. However, after 1996, the LZB experienced significant erosion at the offshore area.

The northern abandoned delta lobe was dominated by wave process following the cutoff of sediment supply in 1976, and mass movement related erosion process may play an important role in the geomorphology development. The evolution of the active delta lobe was controlled by the interaction ofriver sediment load, channel geometry, tidal current and shear front, as well as storm waves and wind-driven currents. The erosion and accumulation in the LZB was closely related to the division of the river channel and the sediment dispersal pattern.

ACKNOWLEDGEMENTS

We appreciate the valuable comments from the editor and two anonymous reviewers. This work was supported by the NSFC projects (Grant No. 41476069, 41525021 and 41376096) and the Fundamental Research Funds for the Central Universities.

LITERATURE CITED

Bi, N. S.; Wang, H. J., and Yang, Z. S., 2014. Recent changes in the erosion-accretion patterns of the active Huanghe (Yellow River) delta lobe caused by human activities. *Continental Shelf Research*, 90(0), 70–78.

Bi, N. S.; Yang, Z. S.; Wang, H. J.; Hu, B. Q, and Ji, Y. J.,

2010. Sediment dispersion pattern off the present Huanghe (Yellow River) subdelta and its dynamic mechanism during normal river discharge period. *Estuarine, Coastal and Shelf Science*, 86(3), 352-362.

Bianchi, T. S. and Allison, M. A., 2009. Large-river delta-front estuaries as natural "recorders" of global environmental change. *Proceedings of the National Academy of Sciences*, 106 (20), 8085-8092.

Bornhold, B. D.; Yang, Z. S.; Keller, G. H.; Prior, D. B.; Wiseman Jr., W. J.; Wang, Q.; Wright, L. D.; Xu, W. D., and Zhuang, Z. Y., 1986. Sedimentary framework of the modern Huanghe (Yellow River) delta. *Geo-Marine Letters*, 6 (2), 77-83.

Chen, S. L.; Zhang, G. A.; Chen, X. Y.; Chen, J. H., and Xu, C. L., 2005a. Coastal erosion feature and mechanism at Feiyantan in the Yellow River delta. *Marine Geology and Quaternary Geolog*, 25 (3), 9 - 14. (In Chinese with English abstract).

Chen, X. Y.; Chen, S. Y.; Li, J. F., and Xu, C. L., 2005b. Study on the Coastal Erosion mechanism in the Yellow River Delta Gudong and Xintan Areas. *Coastal Engineering*, 24 (4), 1-10. (In Chinese with English abstract).

Cheng, Y. J. and Cheng, J. G., 2000. Analysis of the current field in the new Yellow River entrance sea area. *Coastal Engineering*, 19(4), 5-11. (In Chinese with English abstract).

Chu, Z. X.; Sun, X. G.; Zhai, S. K., and Xu, K. H., 2006. Changing pattern of accretion/erosion of the modern Yellow River (Huanghe) subaerial delta, China: Based on remote sensing images. *Marine Geology*, 227(1-2), 13-30.

Cui, B. L. and Li X. Y., 2011. Coastline change of the Yellow River estuary and itsresponse to the sediment and runoff (1976-2005). *Geomorphology*, 127(1-2), 32-40.

Hu, C. H.; Ji, Z. W., and Wang, T., 1996. Characteristics of ocean dynamics and sediment diffusion in the Yellow River estuary. *Journal of Sediment Research*, 4, 2-11. (In Chinese with English abstract).

Hu, C. H. and Cao, W. H., 2003. Variation, regulation and control of flow and sediment in the Yellow River Estuary: I. Mechanism of flow-sediment transport and evolution. *Journal of Sediment Research*, 5, 1-8. (In Chinese with English abstract).

Jia, Y. G.; Liu, X. L.; Shan, H. X.; Zhang, J. W., and Huo, S. X., 2011. The effects of hydrodynamic conditions on geotechnical strength of the sediment in Yellow River Delta. *International Journal of Sediment Research*, 26(3), 318-330.

Kim, S. Y.; Yasuda, T., and Mase, H., 2008, Numerical analysis of effects of tidal variations on storm surges and waves. *Applied Ocean Research*, 30(4), 311-322.

Milliman, J. D. and Meade, R. H., 1983. World-wide delivery of river sediment to the oceans. *Journal of Geology*, 91(1), 1-21.

Li, G. X.; Wei, H. L.; Yue, S. H.; Cheng, Y. J., and Han, Y. S., 1998. Sedimentation in the Yellow River delta, part II: suspended sediment dispersal and deposition on the subaqueous delta. *Marine Geology*, 149(1-4), 113-131.

Li, G. X.; Yang, Z. S.; Yue, S. H.; Zhuang, K. L., and Wei, H. L., 2001. Sedimentation in the shear front off the Yellow River mouth. *Continental Shelf Research*, 21 (6 - 7), 607 -625.

Li, G., X.; Zhuang, K. L., and Wei, H. L., 2000. Sedimentation in the Yellow River delta. Part III. Seabed erosion and diapirism in the abandoned subaqueous delta lobe. *Marine Geology*, 168(1-4), 129-144.

Liu, X. L.; Jia, Y. G.; Zheng, J. W.; Hou, W.; Zhang, L.; Zhang, L. P., and Shan, H. X., 2013. Experimental evidence of wave-induced inhomogeneity in the strength of silty seabed sediments: Yellow River Delta, China. *Ocean Engineering*, 59(0), 120-128.

Liu, Y.; Li, G. X.; Deng, S. G.; Zhao, D. B., and Wen, G. Y., 2002. Evolution of erosion and accumulation in the abandoned subaqueous delta lobe of the Yellow River. *Marine Geology & Quaternary Geology*, 22 (3), 27 - 34. (In Chinese with English abstract).

Overeem, I. and Syvitski, J. P. M., 2009. Dynamics and Vulnerability of Delta Systems. Geesthacht, Schleswig-Holstein, Germany: GKSS Research Center, LOICZ Reports & Studies No. 35, 54p.

Pang, J. Z. and Jiang, M. X., 2003. On the evolution of the Yellow River estuary: - I. Hydrographic characteristics. *Transactions of Oceanology and Limnology*, 2003(3), 1-13. (In Chinese with English abstract).

Pang, J. Z. and Si, S. H., 1980. Fluvial process of the Huanghe River Estuary II - Hydrographical character and the region of sediment silting. *Oceanologia Et Limnologia Sinica*, 11(4), 295-305. (In Chinese with English abstract).

Pelling, H. E.; Uehara, K., and Green, J. A. M., 2013. The impact of rapid coastline changes and sea level rise on the tides in the Bohai Sea, China. *Journal of Geophysical Research: Oceans*, 118(7), 3462-3472.

Prior, D. B.; Suhayda, J. N.; Lu, N. Z.; Bornhold, B. D.; Keller, G. H.; Wiseman, W. J.; Wright, L. D., and Yang, Z. S., 1989. Storm wave reactivation of a submarine landslide. *Nature*, 341(6237), 47-50.

Qiao, L. L.; Bao, X. W.; Wu, D. X., and Wang, X. H., 2008. Numerical study of generation of the tidal shear front off the Yellow River mouth. *Continental Shelf Research*, 28 (14), 1782-1790.

Qiao, S.; Shi, X. F.; Zhu, A. M.; Liu, Y. G; Bi, N. S.; Fang, X. S., and Yang, G., 2010. Distribution and transport of suspended sediments off the Yellow River (Huanghe) mouth and the nearby Bohai Sea. Estuarine, *Coastal and Shelf Science*, 86(3), 337-344.

Wiseman, W. J.; Yang, Z. S.; Bornhold, B. D.; Keller, G. H.; Prior, D. B., and Wright, L. D., 1986. Suspended sediment advection by tidal currents off the Huanghe delta. *GeoMarine Letters*, 6 (2), 107-113.

Saito, Y.; Yang, Z. S., and Hori, K., 2001. The Huanghe (Yellow River) and Changjiang (Yangtze River) deltas: a review on their characteristcs, evolution and sediment discharge during the Holocene. *Geomorphology*, 41 (2 - 3), 219-231.

State Oceanic Administration, 2012. China Sea Level Bulletin. http: // www. mlr. gov. cn/zwgk/tjxx/201303/t20130322 _ 1194292. htm.

Syvitski, J. P. M.; Kettner, A. J.; Hannon, M. T.; Hutton, E. W. H.; Overeem, I.; Brakenridge, G. R.; Day, J.; Vörösmarty, C.; Saito, Y.; Giosan, L., and Nicholls, R. J., 2009. Sinking deltas due to human activities. *Nature Geosci-*

ence, 2(10), 681–686.

Syvitski, J. P. M.; Kettner, A. J.; Correggiari, A., and Nelson, B. W., 2005. Distributary channels and their impact on sediment dispersal. 2005. In: Trincardi, F., and Syvitski, J. (eds), Mediterranean Prodelta Systems. *Marine Geology*, Special Issue 222–223, pp. 75–94.

Wang, H. J; Yang, Z. S.; Saito, Y.; Liu, J. P.; Sun, X. X., and Wang, Y., 2007a. Stepwise decreases of the Huanghe (Yellow River) sediment load (1950–2005): Impacts of climate change and human activities. *Global and Planetary Change*, 57(3–4), 331–354.

Wang, H. J.; Bi, N. S.; Saito, Y.; Wang, Y.; Sun, X. X.; Zhang, J., and Yang, Z. S., 2010. Recent changes in sediment delivery by the Huanghe (Yellow River) to the sea: causes and environmental implications in its estuary. *Journal of Hydrology*, 391(3–4), 302–313.

Wang, H. J.; Yang, Z. S.; Li, G. X., and Jiang, W. S., 2006. Wave climate modeling on the abandoned Huanghe (Yellow River) delta lobe and related deltaic erosion. *Journal of Coastal Research*, 22 (4), 906–918.

Wang, H. J.; Yang, Z. S.; Li, Y. H.; Guo, Z. G.; Sun, X. X., and Wang, Y., 2007b. Dispersal pattern of suspended sediment in the shear frontal zone off the Huanghe (Yellow River) mouth. *Continental Shelf Research*, 27(6), 854–871.

Wei, X. Y.; Ma, Y. Y., and Li, G. X., 2013. Evolution of the Qingshuigou subaqueous delta lobe of Yellow River. *Marine Geology & Quaternary Geology*, 33(1), 19–24. (In Chinese with English abstract).

Wiseman, W.; Fan, Y. B.; Bornhold, B.; Keller, G.; Su, Z. Q.; Prior, D.; Yu, Z. X.; Wright, L.; Wang, F. Q., and Qian, Q. Y., 1986. Suspended sediment advection by tidal currents off the Huanghe (Yellow River) delta. *Geo-Marine Letters*, 6 (2), 107–113.

Wright, L. D. and Nittrouer, C. A., 1995. Dispersal of river sediments in coastal seas: six contrasting cases. *Estuaries*, 18 (3), 494–508.

Wright, L. D.; Short, A. D., and Green, M. O., 1985. Short-term changes in the morphodynamic states of beaches and surf zones: An empirical predictive model. *Marine Geology*, 62(3–4), 339–364.

Wright, L. D.; Yang, Z. S.; Bornhold, B. D.; Keller, G. H.; Prior, D. B., and Wiseman, W. J., 1986. Hyperpycnal plumes and plumes front over the Huanghe delta front. *Geo-Marine Letters*, 6(2), 97–105.

Yang,Z. S.; Ji, Y. J.; Bi, N. S.; Lei, K., and Wang, H. J., 2011. Sediment transport off the Huanghe (Yellow River) delta and in the adjacent Bohai Sea in winter and seasonal comparison. *Estuarine, Coastal and Shelf Science*, 93(3), 173–181.

Ying, M.; Li, J. F.; Chen, S. L.; Li, W. H., and Dai, Z. J., 2008. Dynamics Characteristcs and Topographic Profiles Shaping Process of Feiyantan at the Yellow River Delta. *Marine Science Bulletin*, 26(4), 13–22.

Zang, Q. Y., 1996. Nearshore Sediment along the Yellow River Delta. Beijing: Ocean Press. (In Chinese with English abstract).

Zhang, J.; Huang; W. W., and Shi, M. C., 1990. Huanghe (Yellow River) and its estuary: sediment origin, transport and deposition. *Journal of Hydrology*, 120 (1–4), 203–223.